

# Mitochondria regulate autophagy by conserved signalling pathways

Martin Graef and Jodi Nunnari\*

Department of Molecular and Cellular Biology, Davis University of California, Davis, CA, USA

**Autophagy is a conserved degradative process that is crucial for cellular homeostasis and cellular quality control via the selective removal of subcellular structures such as mitochondria. We demonstrate that a regulatory link exists between mitochondrial function and autophagy in *Saccharomyces cerevisiae*. During amino-acid starvation, the autophagic response consists of two independent regulatory arms—autophagy gene induction and autophagic flux—and our analysis indicates that mitochondrial respiratory deficiency severely compromises both. We show that the evolutionarily conserved protein kinases Atg1, target of rapamycin kinase complex I, and protein kinase A (PKA) regulate autophagic flux, whereas autophagy gene induction depends solely on PKA. Within this regulatory network, mitochondrial respiratory deficiency suppresses autophagic flux, autophagy gene induction, and recruitment of the Atg1–Atg13 kinase complex to the pre-autophagosomal structure by stimulating PKA activity. Our findings indicate an interrelation of two common risk factors—mitochondrial dysfunction and autophagy inhibition—for ageing, cancerogenesis, and neurodegeneration.**

*The EMBO Journal* (2011) 30, 2101–2114. doi:10.1038/emboj.2011.104; Published online 5 April 2011

**Subject Categories:** membranes & transport; cellular metabolism

**Keywords:** autophagy regulation; mitochondria; protein kinase A; TOR

## Introduction

Autophagy is a highly conserved and regulated process essential for the degradation of long-lived proteins and organelles in eukaryotic cells. During autophagy, cytosolic content is sequestered via *de novo* formation of double-membrane-bounded structures termed autophagosomes. The autophagosomal outer membrane docks and fuses with the vacuole and the inner membrane vesicle is subsequently released and degraded by resident hydrolases to generate metabolic building blocks for biosynthesis. In yeast, the autophagy machinery comprised ~30 autophagy-related (ATG) genes, including highly conserved core components. Most Atg proteins dynamically assemble in a hierarchical

manner at pre-autophagosomal structures (PAS), which are putative sites for autophagosome formation (Suzuki *et al*, 2007; Xie and Klionsky, 2007; Kawamata *et al*, 2008; Cebollero and Reggiori, 2009; He and Klionsky, 2009; Nakatogawa *et al*, 2009).

The extent and rate of autophagy are controlled by the availability of nutrients. Starvation strongly induces autophagy and this regulation is essential for long-term cellular survival (Takeshige *et al*, 1992; Tsukada and Ohsumi, 1993; Komatsu *et al*, 2005). Multiple signalling pathways regulate autophagy including the conserved serine/threonine protein kinase target of rapamycin kinase complex I (TORC1) and cAMP-dependent protein kinase A (PKA) pathways, which also sense nutrient availability and control cellular growth (Noda and Ohsumi, 1998; Budovskaya *et al*, 2004; Yorimitsu *et al*, 2007, 2009; Stephan *et al*, 2009; Yang *et al*, 2010). In yeast, TORC1 and PKA negatively regulate autophagy at least in part by directly and independently phosphorylating the conserved kinase Atg1 (ULK1/2 in mammals) and Atg13 (mammalian Atg13), and by blocking the assembly and localization of an active Atg1–Atg13 complex to the PAS. Localization of an active Atg1–Atg13 complex to the PAS is required to initiate autophagosome formation and subsequent vacuolar turnover or autophagic flux (Budovskaya *et al*, 2005; Kabeya *et al*, 2005; Chan *et al*, 2007; Cheong *et al*, 2008; Hara *et al*, 2008; Stephan *et al*, 2009; Kamada *et al*, 2010).

Autophagy is also regulated via the transcriptional up-regulation or induction of autophagy genes by ill-defined mechanisms (Abeliovich *et al*, 2000). In yeast, starvation induces the transcription of *ATG1* and *ATG13* as well as *ATG14*, which encodes a component of the phosphatidylinositol-3 kinase complex I (Hardwick *et al*, 1999; Chan *et al*, 2001). *ATG8*, which encodes an ubiquitin-like PAS-localized protein required for autophagosome formation, and the genes encoding the Atg8 ubiquitin-like modification system (*ATG3*, *ATG4*, *ATG5*, *ATG7*, and *ATG12*) are also transcriptionally regulated during starvation (Hardwick *et al*, 1999; Kirisako *et al*, 1999; Huang *et al*, 2000). Induction of this *ATG8* module is functionally relevant, as the level of Atg8 has been shown to determine the size of forming autophagosomes and, thus, to positively influence the magnitude of the autophagic response (Abeliovich *et al*, 2000; Xie *et al*, 2008).

Although autophagy is considered non-specific in yeast, selective forms have been described including receptor-mediated targeting of the autophagy machinery to mitochondria (mitophagy), but the functional role of mitophagy in yeast is not known (Kissova *et al*, 2004, 2007; Tal *et al*, 2007; Kanki *et al*, 2009; Okamoto *et al*, 2009). In mammalian cells, the selective autophagic removal of depolarized mitochondria is consistent with a quality control mechanism (Priault *et al*, 2005; Nowikovsky *et al*, 2007; Narendra *et al*, 2008, 2010; Twig *et al*, 2008; Geisler *et al*, 2010; Suen *et al*, 2010; Vives-Bauza *et al*, 2010). A connection between autophagy and maintenance of mitochondrial function is also implied by the fact that defects in either are associated with a set of

\*Corresponding author. Department of Molecular and Cellular Biology, Davis University of California, 3220 Briggs Hall/LSA, Davis, CA 95616-8535, USA. Tel.: +1 530 754 9774; Fax: +1 530 752 7522; E-mail: jmnunnari@ucdavis.edu

Received: 12 July 2010; accepted: 16 March 2011; published online: 5 April 2011

common, but diverse diseases, such as cancer, ageing, and neurodegeneration (Hara *et al.*, 2006; Komatsu *et al.*, 2006; Huang and Klionsky, 2007; Banerjee *et al.*, 2009; Meijer and Codogno, 2009; Morselli *et al.*, 2009; Cardoso *et al.*, 2010; Galluzzi *et al.*, 2010; Lee *et al.*, 2010; Wong and Cuervo, 2010). Alternatively, the common denominator of autophagy and mitochondria in disease might be that mitochondrial dysfunction directly affects and regulates the autophagy capacity of eukaryotic cells. We addressed this latter possibility in *Saccharomyces cerevisiae* and demonstrate that an intimate link exists between mitochondrial function and autophagy regulation during amino-acid starvation.

## Results

### Mitochondrial respiratory deficiency impairs autophagy gene induction and autophagic flux

We investigated the role of mitochondria in the regulation of autophagy by monitoring the behaviour of the GFP-Atg8 reporter under the control of the endogenous *ATG8* promoter in yeast (pRS416-pr<sup>ATG8</sup>-GFP-*ATG8*) (Abeliovich *et al.*, 2003). Using this reporter, we assayed two critical components of the autophagic response: autophagic flux and *ATG8* induction (Kirisako *et al.*, 1999; Abeliovich *et al.*, 2000; Shintani and Klionsky, 2004; Xie *et al.*, 2008). Autophagic flux, which is the vacuolar transfer and degradation of autophagosomes over time, was quantified by measuring the vacuolar degradation of the Atg8 domain of the reporter (ratio of free GFP to total GFP signal) over time by western blot analysis (Shintani and Klionsky, 2004). Similarly, we measured *ATG8* induction by quantifying the fold increase of total GFP signal (GFP-Atg8 and free GFP signal) normalized to a non-induced protein (Cdc11). In addition, *ATG8* induction was monitored independently from autophagic flux using a GFP-only reporter under the control of the endogenous *ATG8* promoter (pRS426-pr<sup>ATG8</sup>-GFP).

To examine the role of mitochondria, we compared the autophagic response under starvation conditions of wild-type cells to wild-type cells lacking mitochondrial genomes ( $\rho^0$  cells). Cells were grown in galactose as opposed to glucose as a carbon source to allow fermentative growth of respiratory-deficient  $\rho^0$  cells without glucose repression of mitochondrial biogenesis. Subsequently, autophagy was induced by exposing cells to amino-acid starvation, which was faithfully produced using a relatively low concentration of yeast extract (0.1% (w/v)) (Supplementary Figure S1) or standard nitrogen starvation conditions. We also varied the carbon source during amino-acid starvation to determine the degree to which the autophagic response depends on mitochondrial function. Specifically, we examined the effects of no carbon source (carbon starvation); acetate as a non-fermentable carbon source; and galactose or glucose as fermentable carbon sources that are non-repressive or repressive for mitochondrial biogenesis, respectively.

Analysis of wild-type and  $\rho^0$  cells indicates that under amino-acid starvation, *ATG8* induction was strictly dependent on both the presence of a carbon source and mitochondrial function (Figure 1A, *ATG8* induction). Specifically, we found that in the absence of a carbon source, neither wild-type nor  $\rho^0$  cells displayed significant *ATG8* induction (Figure 1A, no carbon). In contrast, in the presence of the non-fermentable carbon source acetate or the fermentable carbon sources

galactose and glucose, *ATG8* expression in wild-type cells was significantly stimulated (Figure 1A, acetate, galactose, or glucose). Remarkably, we did not observe any *ATG8* induction in  $\rho^0$  cells in the presence of either non-fermentable or fermentable carbon sources, demonstrating that mitochondrial respiratory deficiency blocks *ATG8* induction in response to amino-acid starvation (Figure 1A).

To test whether mitochondrial function also regulates the expression of other key autophagy factors under amino-acid starvation, we analysed *ATG14*, which encodes another highly induced essential component of the autophagy machinery (Chan *et al.*, 2001). We analysed the expression of a plasmid-encoded GFP reporter under the control of the endogenous *ATG14* promoter in wild-type,  $\rho^0$ , and *Δatg7* cells. In wild-type and *Δatg7* cells, we observed a strong induction of the *ATG14* promoter-driven GFP reporter upon amino-acid starvation (Supplementary Figure S2). Importantly, *ATG14* induction was completely absent in  $\rho^0$  cells (Supplementary Figure S2), indicating that mitochondrial function is a more general regulator of expression-regulated autophagy components. Interestingly, we observed a slightly elevated basal level of *ATG14* promoter-controlled GFP expression in  $\rho^0$  cells (0 h starvation) as compared with wild-type cells that might reflect compensatory adaptations to mitochondrial dysfunction (Supplementary Figure S2).

In contrast to *ATG8* induction, autophagic flux was not dependent on carbon source in wild-type cells during amino-acid starvation (Figure 1A, autophagic flux). In  $\rho^0$  cells, however, autophagic flux was significantly decreased in comparison with wild-type cells, even in the presence of galactose or glucose (Figure 1A, galactose or glucose), but the extent of inhibition varied with the type of carbon source (Figure 1A). These observations indicate that the strong defect in the overall autophagic response observed in respiratory-deficient cells is due to a combined inhibitory effect on both *ATG8* induction and autophagic flux. Interestingly, wild-type and  $\rho^0$  cells starved for all nitrogen sources instead of only amino acids displayed an indistinguishable autophagic flux (Figure 1A, glucose (-N)). This demonstrates that the defects in autophagic flux observed in  $\rho^0$  cells under amino-acid starvation are not due to intrinsic defects in the autophagy machinery or in vacuolar biogenesis. This conclusion is consistent with published data, indicating that vacuolar morphology and acidification is normal in  $\rho^0$  cells (Chen *et al.*, 2008) and is further supported by our phenotypic analysis showing that  $\rho^0$  cells are resistant to stress conditions that inhibit growth of a vacuolar acidification mutant (*Δvma2*) (Supplementary Figure S3). However, as with amino-acid starvation, a severe defect in *ATG8* induction was observed in  $\rho^0$  cells under nitrogen starvation in comparison with the three-fold induction of *ATG8* in wild-type cells, which is consistent with published results (Figure 1A) (Kirisako *et al.*, 1999; Huang *et al.*, 2000). These findings indicate that there are differences in the regulation of autophagy under amino-acid versus nitrogen starvation conditions, consistent with recently published work, indicating a differential role for Gcn2 and Gcn4 in autophagy regulation in response to amino-acid and nitrogen starvation (Ecker *et al.*, 2010). Importantly, our data point to an essential role for mitochondrial function in *ATG8* induction and the autophagic response.

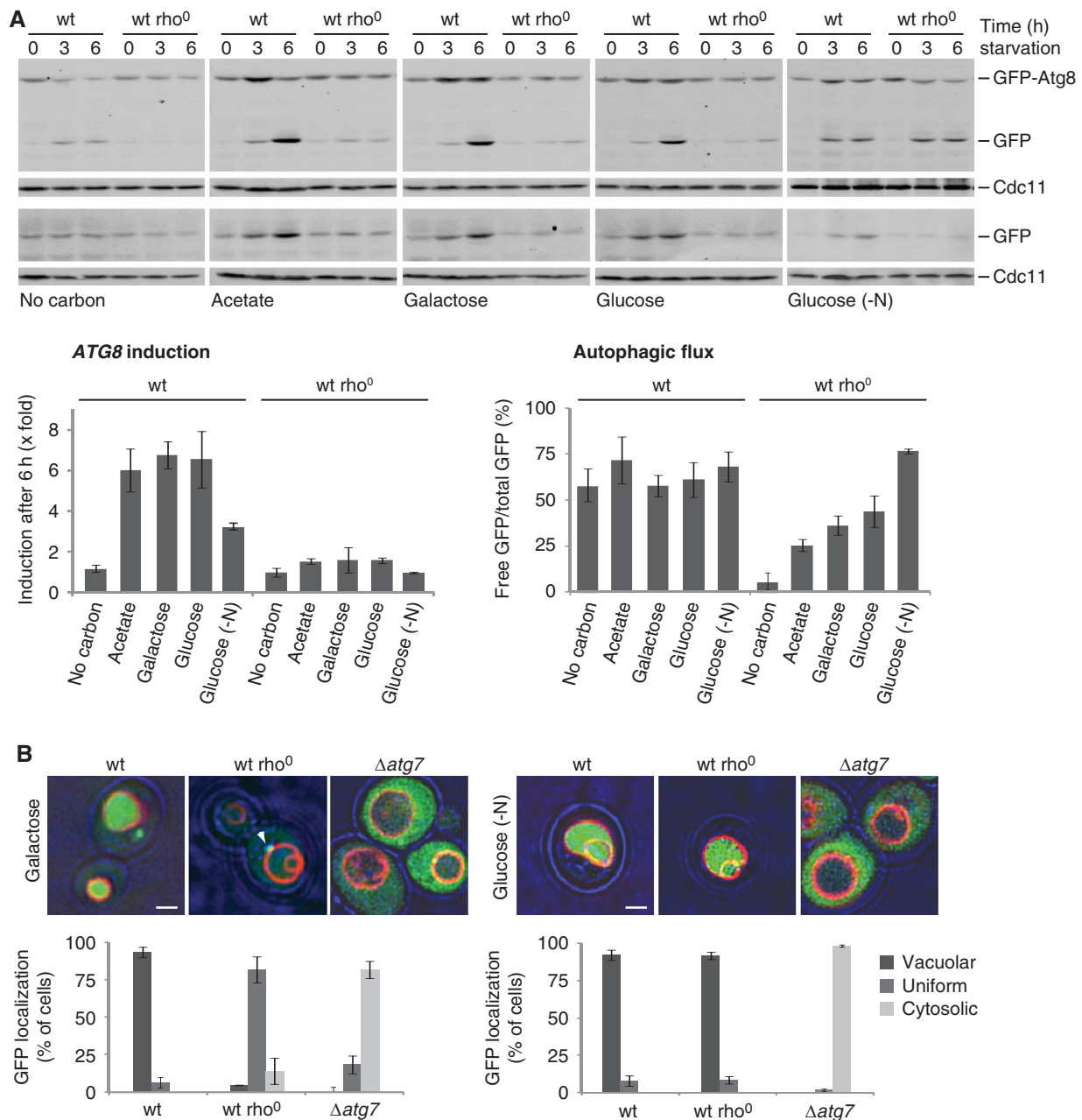


**Figure 1** Mitochondrial respiratory deficiency impairs *ATG8* induction and autophagic flux. **(A)** Wild-type and rho<sup>0</sup> cells harbouring pr<sup>ATG8</sup>-GFP-*ATG8* (upper panels) or pr<sup>ATG8</sup>-GFP (lower panels) were exposed to amino-acid or nitrogen starvation (-N) medium supplemented with indicated carbon sources. Cells were analysed at indicated time points by whole cell extraction and western blot analysis using  $\alpha$ -GFP and  $\alpha$ -Cdc11 antibodies. Quantification of *ATG8* induction is shown in the lower left panel. Total GFP signals (GFP-*ATG8* and free GFP) were quantified and normalized to Cdc11 signals. Normalized values at 0 h were set as one and relative changes are shown after 6 h starvation. Quantification of autophagic flux is shown in the lower right panel as ratio of free GFP to total GFP signals (GFP-*ATG8* and free GFP) after 6 h starvation. The means and s.d. of four ( $n=4$ ) independent experiments are indicated. **(B)** Fluorescence microscopical analysis. Wild-type, rho<sup>0</sup>, and  $\Delta atg7$  cells expressing pr<sup>ATG8</sup>-GFP-*ATG8* were grown as described in **(A)** and exposed to amino-acid (left panel, galactose) or nitrogen starvation (right panel, glucose (-N)) for 6 h. Vacuoles were visualized by over night FM4-64 (1  $\mu$ M) staining (red). Arrowhead indicates a punctate GFP-*ATG8* structure. Transmission and fluorescence light microscopy images were superimposed to visualize cellular boundaries. Cellular localization of GFP signal was analysed in at least 150 cells ( $n \geq 150$ ) for each strain and condition. Scale bars represent 1.5  $\mu$ m.

To further substantiate our conclusions, we analysed GFP-*ATG8*-expressing cells by fluorescence microscopy. Consistently, under amino-acid starvation, wild-type cells exhibited a strong vacuolar GFP signal, as assessed by the vital vacuolar dye FM4-64, that was dependent on the essential autophagy component, Atg7, indicating autophagic turnover of GFP-*ATG8* (Figure 1B) (Tanida *et al*, 1999; Huang

*et al*, 2000). In contrast, in rho<sup>0</sup> cells under identical conditions, a uniformly distributed weak GFP signal was observed, which supports our biochemical data showing impaired *ATG8* induction and autophagic flux in rho<sup>0</sup> cells (Figure 1B, galactose). GFP-*ATG8* was observed in punctate structures in amino-acid starved rho<sup>0</sup> cells (Figure 1B, galactose), raising the possibility that Atg8 recruitment to the PAS is not affected

(Kirisako *et al*, 1999). In contrast, under nitrogen starvation,  $\rho^0$  cells displayed a vacuolar GFP signal, which indicates autophagic turnover under these conditions—a conclusion also supported by our biochemical analysis (Figure 1A and B). Together, these data indicate that *ATG8* induction and autophagic flux are differentially regulated and demonstrate that mitochondria have important roles in both *ATG8* induction and in the modulation of autophagic flux in the autophagic response to amino-acid starvation.

We also tested whether mitochondrial function regulates autophagy induced during stationary phase. Wild-type cells displayed a significant autophagic response after 2–4 days in stationary phase (Supplementary Figure S4). Autophagic flux was blocked in  $\Delta atg7$  cells as expected; however, *ATG8* induction was observed (Supplementary Figure S4). In contrast, we did not detect either autophagic flux or *ATG8* induction in  $\rho^0$  cells under these conditions (Supplementary Figure S4). Thus, mitochondrial function is a general regulator of the autophagic response.

### Characterization of the role of mitochondria in the autophagic response

The  $\rho^0$  cells lack the mitochondrial-encoded core subunits of the respiratory chain and mitochondrial  $F_1F_0$ -ATP synthase and are, therefore, unable to utilize non-fermentable carbon sources to generate a proton gradient across the inner mitochondrial membrane or produce ATP by respiration. To determine whether specific defects in the respiratory chain complex III (CIII), complex IV (CIV), or in the  $F_1F_0$ -ATP synthase (CV) are linked to the regulation of autophagy, we compared autophagy induction in wild-type,  $\rho^0$ , and  $\Delta atg7$  cells with cells that maintain mtDNA, but are selectively impaired in CIII, CIV, or CV activity. Specifically, CIII was blocked in wild-type cells by the addition of the selective inhibitor antimycin A or in a mutant lacking *Cbs1* ( $\Delta cbs1$ ), a nuclear-encoded factor specifically required for the translation of *Cob1*, the mitochondrial-encoded core subunit of CIII (Rodel, 1997). Similarly, CIV function was impaired in mutants lacking the nuclear-encoded factors *Mss51* ( $\Delta mss51$ ), *Pet111* ( $\Delta pet111$ ), or *Pet122* ( $\Delta pet122$ ) required for the translation of the mitochondrial-encoded CIV core subunits *Cox1*, *Cox2*, or *Cox3*, respectively (Poutre and Fox, 1987; Costanzo and Fox, 1988; Decoster *et al*, 1990; Herrmann and Funes, 2005). CV activity was inhibited in wild-type cells by the addition of the selective inhibitor oligomycin or in a mutant lacking *Atp10* ( $\Delta atp10$ ), a nuclear-encoded factor required for the assembly of the  $F_0$ -sector of  $F_1F_0$ -ATP synthase (Ackerman and Tzagoloff, 1990; Tzagoloff *et al*, 2004). We analysed autophagy in the presence of the non-fermentable carbon source acetate or the non-repressive fermentable carbon source galactose during amino-acid starvation to vary dependence on mitochondrial function.

In the presence of the non-fermentable carbon source acetate, inhibition of CIII, CIV, or CV blocked the induction of *ATG8* expression and autophagic flux in response to amino-acid starvation to a similar degree as observed in  $\rho^0$  cells (Figure 2A). Similarly, induction of *ATG14* was strongly inhibited in the presence of antimycin A or oligomycin under these conditions (Supplementary Figure S2). Thus, respiratory activity that results in the production of mitochondrial ATP is required for the autophagic response under amino-acid starvation in the presence of a non-fermentable

carbon source. Significantly, in the presence of the fermentable carbon source galactose, inhibition of CIII or CIV had different effects on the autophagic response as compared with those observed upon inhibition of the  $F_1F_0$ -ATP synthase (CV). Specifically, a block of CIII or CIV activity strongly impaired *ATG8* induction and partially affected autophagic flux in response to starvation (Figure 2B). In contrast, cells inhibited for CV activity displayed over three-fold induction of *ATG8*, which was similar to that observed for untreated wild-type or  $\Delta atg7$  cells, and a level of autophagic flux similar to that observed for wild-type cells (Figure 2B). These data indicate that mitochondrial ATP production *per se* is not required for the autophagic response during amino-acid starvation.

Given our data demonstrating that mitochondrial respiratory activity is a critical regulator of autophagy induction during amino-acid starvation, we investigated the nature of the regulatory signal(s). Inhibition of respiratory complexes has been associated with an increased generation of reactive oxygen species, previously implicated in mammalian autophagy regulation (Scherz-Shouval *et al*, 2007; Lambert and Brand, 2009). However, overexpression of cytosolic (*Sod1*) or mitochondrial (*Sod2*) superoxide dismutase did not affect the autophagy response in wild-type or  $\rho^0$  cells or in wild-type cells treated with antimycin A or oligomycin during amino-acid starvation in the presence of galactose (Supplementary Figure S5A). Thus, ROS do not have a significant role under these conditions.

Next, we tested whether ATP levels and/or mitochondrial membrane potential could function as mitochondrial signals for autophagy regulation during amino-acid starvation. Therefore, we examined the effects of mitochondrial respiratory deficiency on cellular and mitochondrial ATP levels during amino-acid starvation in the presence of acetate or galactose (Figure 3A and B). In  $\rho^0$  cells, the cellular and mitochondrial ATP levels were significantly lower under growing conditions than those observed in wild-type cells (Figure 3A and B, time 0 h), and did not change during amino-acid starvation in the presence of acetate or galactose (Figure 3A and B, time 3 and 6 h). In contrast, the levels of cellular and mitochondrial ATP significantly decreased in wild-type cells, antimycin A (block of CIII)- or oligomycin (block of CV)-treated wild-type cells, and  $\Delta atg7$  cells during amino-acid starvation (Figure 3A and B, time 0, 3, and 6 h). Interestingly, under all conditions, the reduction of ATP levels occurred independently of mitochondrial function and levels were similar to those observed in  $\rho^0$  cells under both growing and amino-acid starvation conditions. This raises the possibility that regulatory mechanisms exist that maintain ATP levels in a relatively narrow range. Although our data indicate that ATP production is required for the autophagy response during amino-acid starvation (Figure 2A and B), modulation of ATP level was independent of mitochondrial function and, therefore, ATP levels are unlikely to represent a direct mitochondrial signal for autophagy regulation.

During amino-acid starvation in the presence of a fermentable carbon source, *ATG8* induction and, to a lesser extent, autophagic flux require functional CIII and CIV respiratory chain complexes. Blocking the function of these complexes has been correlated with a decrease in mitochondrial membrane potential (Johnson *et al*, 1981; Chen, 1988; Petit *et al*, 1996; Ludovico *et al*, 2001), raising the possibility that

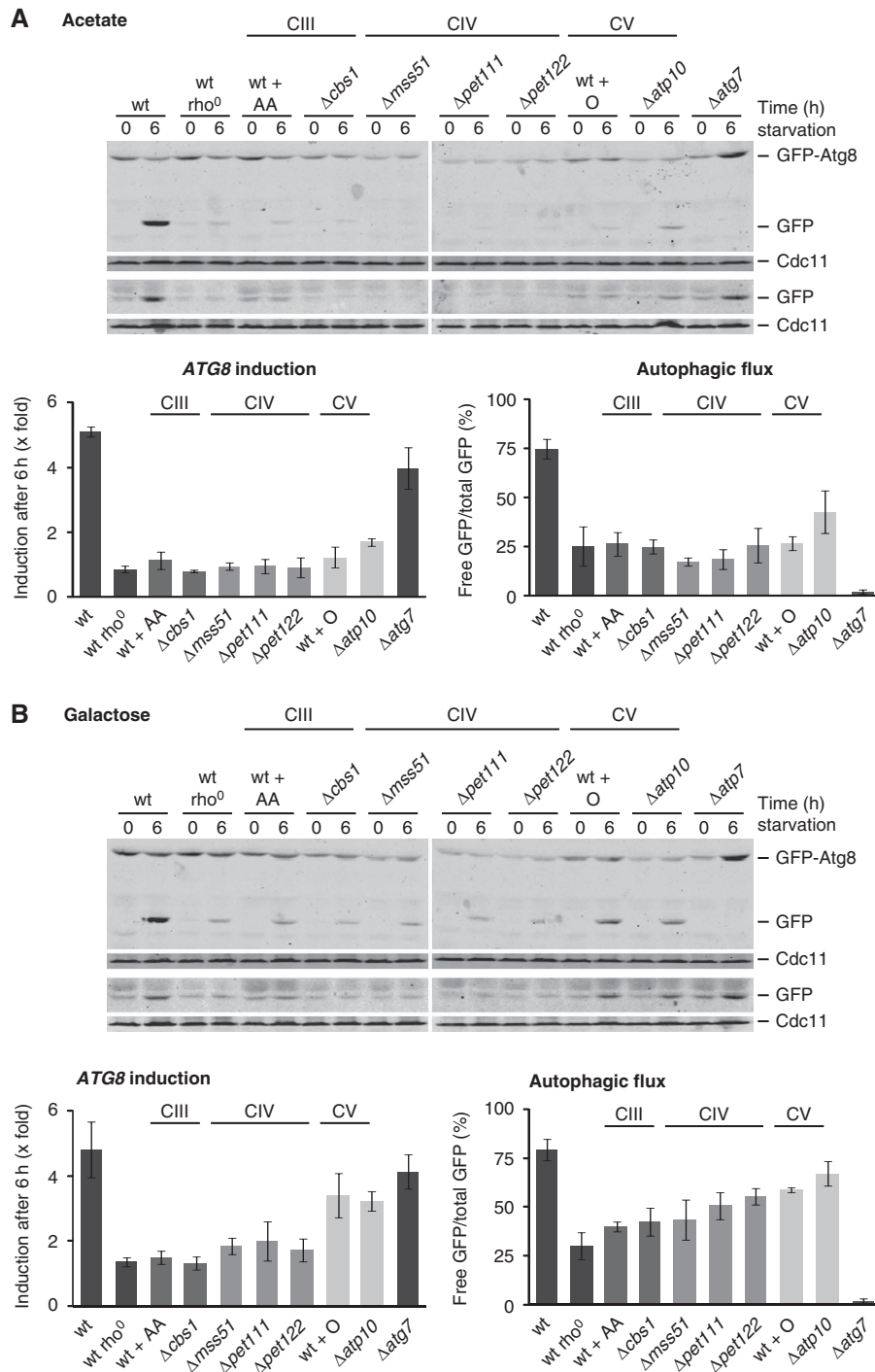


**Figure 2** Autophagic response in cells with compromised respiratory chain complex III, IV, or V activity during amino-acid starvation. Wild-type, rho<sup>0</sup>,  $\Delta atg7$  cells and mutants that are selectively inhibited in the biogenesis of respiratory chain complex III (CIII:  $\Delta cbs1$ ), complex IV (CIV:  $\Delta mss51$ ,  $\Delta pet111$ ,  $\Delta pet122$ ), or the F<sub>1</sub>F<sub>0</sub>-ATP synthase (complex V; CV:  $\Delta atp10$ ) were exposed to amino-acid starvation medium supplemented with acetate (A) or galactose (B). When indicated, wild-type cells were exposed to antimycin A (AA) or oligomycin (O) during the amino-acid starvation period. All strains expressed pr<sup>ATG8</sup>-GFP-ATG8 (upper panels) or pr<sup>ATG8</sup>-GFP (lower panels). Samples were analysed as described in Figure 1A. The means and s.d. of five (n = 5) independent experiments are indicated.

maintenance of a mitochondrial membrane potential by respiration under fermentative amino-acid starvation conditions is required for autophagy induction. To test this possibility, we monitored mitochondrial membrane potential during amino-acid starvation by fluorescence microscopy of living cells using the mitochondrial membrane potential-dependent dye DiOC<sub>3</sub>(6). After 3 h of amino-acid starvation,

wild-type cells treated with antimycin A (block of CIII) showed a strong reduction in DiOC<sub>3</sub>(6) fluorescence compared with wild-type or  $\Delta atg7$  cells in the presence of acetate or galactose as carbon sources, indicating that mitochondrial membrane potential is significantly reduced (Figure 3C). In contrast, oligomycin treatment of wild-type cells (block of CV) resulted in a similar or increased DiOC<sub>3</sub>(6) fluorescence

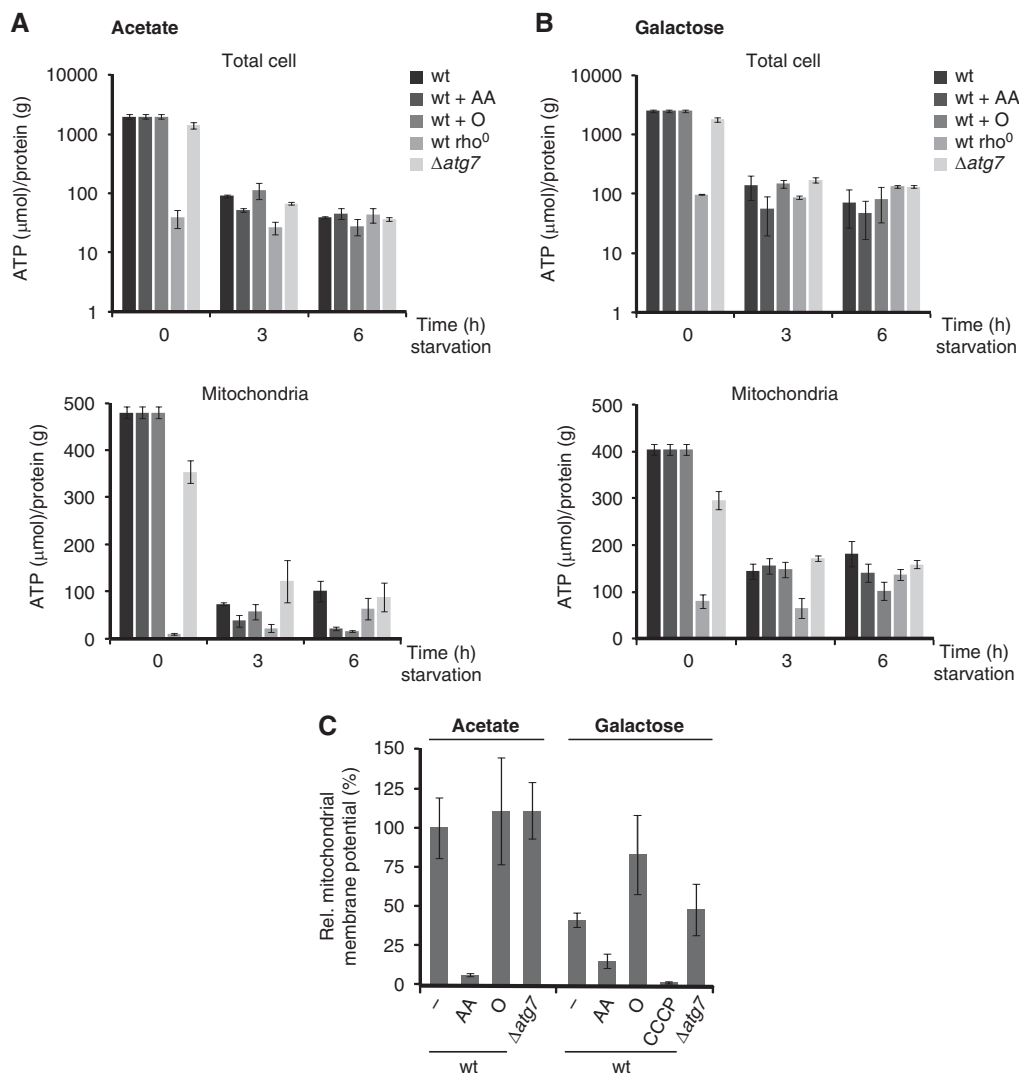


**Figure 3** ATP level and mitochondrial membrane potential during amino-acid starvation. (A, B) Wild-type, rho<sup>0</sup>, and Δatg7 cells were exposed to amino-acid starvation medium supplemented with acetate (A) or galactose (B). When indicated, wild-type cells were exposed to antimycin A (AA) or oligomycin (O) during the amino-acid starvation period. ATP and protein from total cells (upper panels) or isolated mitochondria (lower panels) were determined at indicated time points. (C) Wild-type and Δatg7 cells were exposed to amino-acid starvation medium supplemented with acetate or galactose for 3 h. Wild-type cells were exposed to antimycin A (AA), oligomycin (O), or CCCP (50 μM) during the amino-acid starvation period when indicated. Cells were treated with the mitochondrial membrane potential-dependent dye DiOC<sub>6</sub>(3) and examined by fluorescence microscopy. Average pixel intensities for at least 10 mitochondrial tubules (n = 10) in 5 representative cells were determined for each condition. Values for wild-type mitochondria in the presence of acetate were defined as 100% and relative values were calculated accordingly. The means and s.d. are shown.

compared with untreated wild-type cells in the presence of acetate or galactose, respectively, indicating maintenance of mitochondrial membrane potential (Figure 3C). Hence, mitochondrial defects that result in a reduced mitochondrial membrane potential are correlated with a strong inhibition of the autophagy response, even under fermentative conditions. To substantiate a role for mitochondrial membrane potential changes in the regulation of autophagy, we monitored autophagy induction in wild-type cells in the presence of increasing concentrations of the membrane uncoupler carbonyl cyanide m-chlorophenylhydrazone (CCCP) during amino-acid starvation (Supplementary Figure S5B). As expected, CCCP strongly reduced mitochondrial membrane potential as assessed by DiOC<sub>6</sub>(3) fluorescence and, consistently, impaired the induction of ATG8 in a dose-dependent manner to a similar extent as that observed in rho<sup>0</sup> cells (Figure 3C; Supplementary Figure S5B). Similarly, autophagic

flux was strongly impaired in the presence of CCCP, but we cannot exclude the possibility that CCCP treatment impaired acidification of the vacuole, essential for autophagic turnover (Supplementary Figure S5B) (Nakamura *et al*, 1997). Together, these observations support a model where mitochondrial membrane potential signals the functional state of mitochondria and predominantly modulates the ATG8 induction component of the autophagic response in cells.

### Mitochondria regulate autophagy primarily via PKA

To understand how mitochondria regulate the autophagic response, we assessed the role of two major signalling pathways involved in autophagy regulation. The TORC1 and the cAMP-dependent PKA independently control autophagy by regulating the assembly, activity, and PAS localization of the Atg1-Atg13 complex by direct phosphorylation (Kamada *et al*, 2000, 2010; Budovskaya *et al*, 2005; Stephan *et al*,



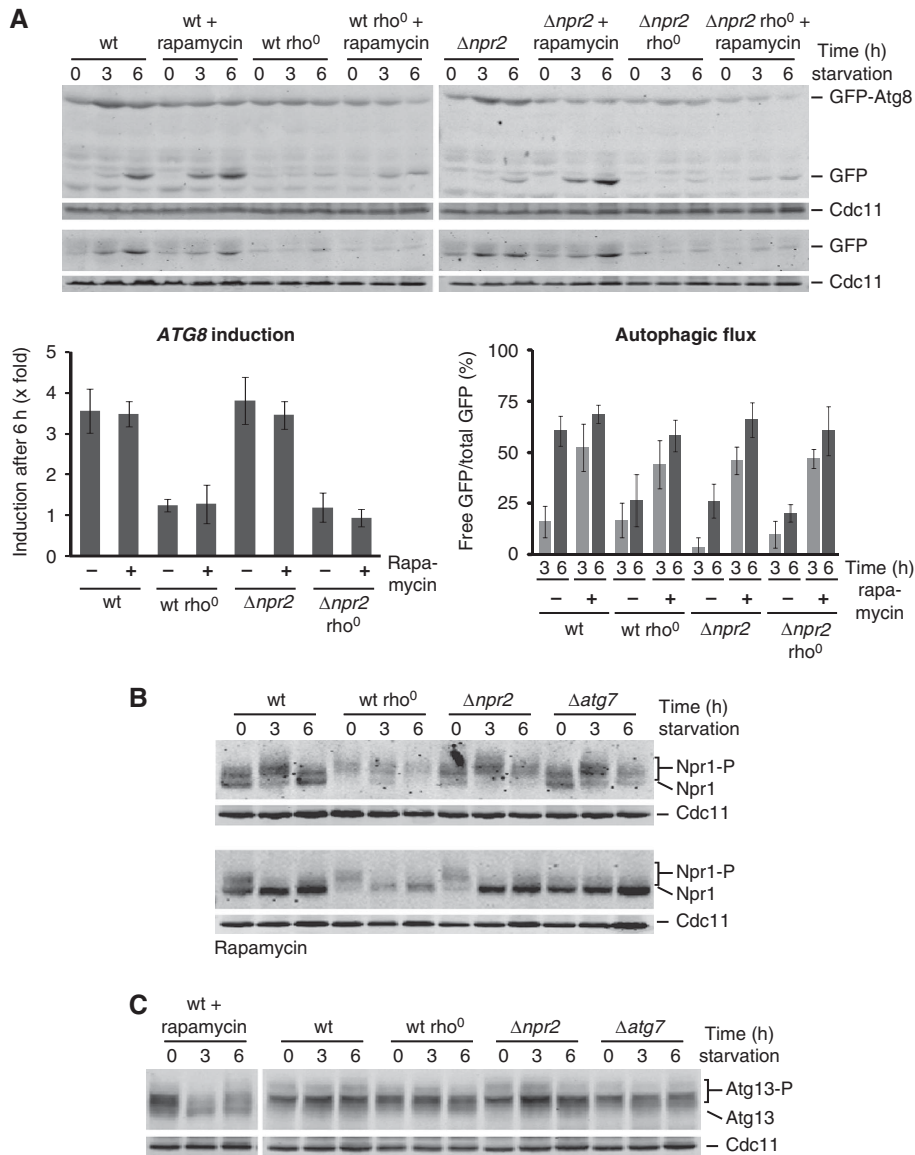


**Figure 4** Role of TORC1 in autophagy regulation under amino-acid starvation. **(A)** Wild-type, rho<sup>0</sup>, Δnpr2, and Δnpr2 rho<sup>0</sup> cells expressing pr<sup>ATG8</sup>-GFP-ATG8 (upper panel) or pr<sup>ATG8</sup>-GFP (lower panel) were exposed to amino-acid starvation medium supplemented with galactose in the absence or presence of rapamycin. Samples were analysed as described in Figure 1A. The means and s.d. of four (n=4) independent experiments are indicated. **(B)** Wild-type, rho<sup>0</sup>, Δnpr2, and Δatg7 cells expressing pr<sup>NPR1</sup>-NPR1-HA were exposed to amino-acid starvation medium supplemented with galactose in the absence (upper panels) or presence (lower panels) of rapamycin. The hyperphosphorylated (Npr1-P) and dephosphorylated (Npr1) forms of Npr1 are indicated. Cells were analysed at indicated time points by whole cell extraction and western blot analysis using α-HA and α-Cdc11 antibodies. **(C)** Wild-type, rho<sup>0</sup>, Δnpr2, and Δatg7 cells were exposed to amino-acid starvation medium supplemented with galactose. Additionally, wild-type cells were treated with rapamycin during starvation (left panel). Phosphorylated (Atg13-P) and dephosphorylated (Atg13) Atg13 was monitored at indicated time points by whole cell extraction and western blot analysis using α-Atg13 and α-Cdc11 antibodies.

2009). TORC1 and PKA activity suppresses both ATG8 induction and autophagic flux, indicating that both are negative regulators of the autophagic response (Noda and Ohsumi, 1998; Budovskaya et al, 2004).

We examined the role of TORC1 in mitochondria-regulated autophagy during amino-acid starvation by monitoring the autophagic response in wild-type, wild-type rho<sup>0</sup>, Δnpr2, and Δnpr2 rho<sup>0</sup> cells in the absence or presence of the TORC1-specific inhibitor rapamycin. NPR2 encodes a component of a conserved Npr2/Npr3 complex recently identified to have a critical role in TORC1 inhibition and cellular adaptation upon amino-acid starvation (Neklesa and Davis, 2009).

Autophagic flux was strongly impaired in the Δnpr2 mutant compared with wild-type cells under amino-acid starvation (Figure 4A), indicating that inhibition of TORC1 via Npr2/3 is critical for the positive regulation of autophagic flux. Consistently, TORC1 inhibition by rapamycin treatment resulted in an indistinguishable autophagic flux in wild-type and Δnpr2 cells (Figure 4A). Interestingly, autophagic flux was significantly accelerated in rapamycin-treated wild-type cells compared with untreated wild-type cells, suggesting that TORC1 is only partially inactivated upon amino-acid starvation (Figure 4A, 3 versus 6 h). Significantly, we observed a similar rapamycin-mediated stimulation of autophagic flux in

$\rho^0$  and  $\Delta npr2 \rho^0$  cells (Figure 4A), indicating that inhibition of TORC1 can suppress decreased autophagic flux caused by mitochondrial respiratory deficiency. It is interesting to note that wild-type and  $\rho^0$  cells displayed remarkably similar autophagic flux during nitrogen starvation in the presence and absence of rapamycin compared with rapamycin-treated cells during amino-acid starvation (Figure 4A; Supplementary Figure S6A). Further, the autophagic response to nitrogen starvation was completely absent in the  $\Delta npr2$  mutant (Supplementary Figure S6A).

To assess TORC1 activity in cells, we monitored phosphorylation of Npr1, a TORC1 effector that is hyperphosphorylated under growing conditions and dephosphorylated under nitrogen starvation or rapamycin treatment in a TORC1-dependent manner (Schmidt *et al.*, 1998; Gander *et al.*, 2008). Although the significance is not clear, the steady-state level of Npr1 was decreased in  $\rho^0$  cells (Figure 4B). More importantly, however, we observed no significant differences in the phosphorylation pattern of Npr1 in wild-type,  $\rho^0$ ,  $\Delta npr2$ , or  $\Delta atg7$  cells during amino-acid starvation (Figure 4B). In contrast, we observed an accumulation of the dephosphorylated form of Npr1 during nitrogen starvation in wild-type,  $\rho^0$ , and  $\Delta atg7$ , indicating a strong inhibition of TORC1 activity (Supplementary Figure S6B). Similarly, upon amino-acid starvation in the presence of rapamycin, we observed a shift towards the dephosphorylated form of Npr1 in all strains (Figure 4B). Consistent with published results, the phosphorylation pattern of Npr1 was unchanged in  $\Delta npr2$  cells during nitrogen starvation (Neklesa and Davis, 2009), but chemical inhibition of TORC1 with rapamycin caused the accumulation of the dephosphorylated Npr1 form. In contrast, rapamycin treatment did not further alter the phosphorylation status of Npr1 in wild-type,  $\rho^0$ , or  $\Delta atg7$  cells (Supplementary Figure S6B). Similarly, the phosphorylation pattern of Atg13 did not change in wild-type,  $\rho^0$ ,  $\Delta npr2$ , or  $\Delta atg7$  cells during amino-acid starvation (Figure 4C). In contrast, a strong decrease in the phosphorylated forms and appearance of the dephosphorylated form of Atg13 were observed in rapamycin-treated wild-type cells, consistent with inhibition of TORC1 (Figure 4C). These data demonstrate a dominant regulatory role for TORC1 activity during nitrogen starvation in contrast to amino-acid starvation and indicate that there are significant differences in autophagy regulation under these two conditions.

In contrast to autophagic flux, *ATG8* induction was not affected in  $\Delta npr2$  cells compared with wild-type cells during amino-acid starvation (Figure 4A). Furthermore, rapamycin-mediated TORC1 inhibition did not alter *ATG8* induction in wild-type or  $\Delta npr2$  cells or the defect in *ATG8* induction caused by mitochondrial dysfunction in  $\rho^0$  and  $\Delta npr2 \rho^0$  cells (Figure 4A). These results indicate that, under amino-acid starvation, the induction of *ATG8* expression is regulated in a TORC1-independent manner. Thus, under conditions of amino-acid starvation, our results support the existence of two regulatory arms of the autophagic response that differentially control autophagic flux and *ATG8* induction in a TORC1-dependent and TORC1-independent manner, respectively. Thus, mitochondria modulate *ATG8* induction via regulatory mechanisms other than TORC1.

We tested whether mitochondria modulate the autophagic response via PKA by performing a comparative analysis of the role of PKA and mitochondrial function in the autophagic

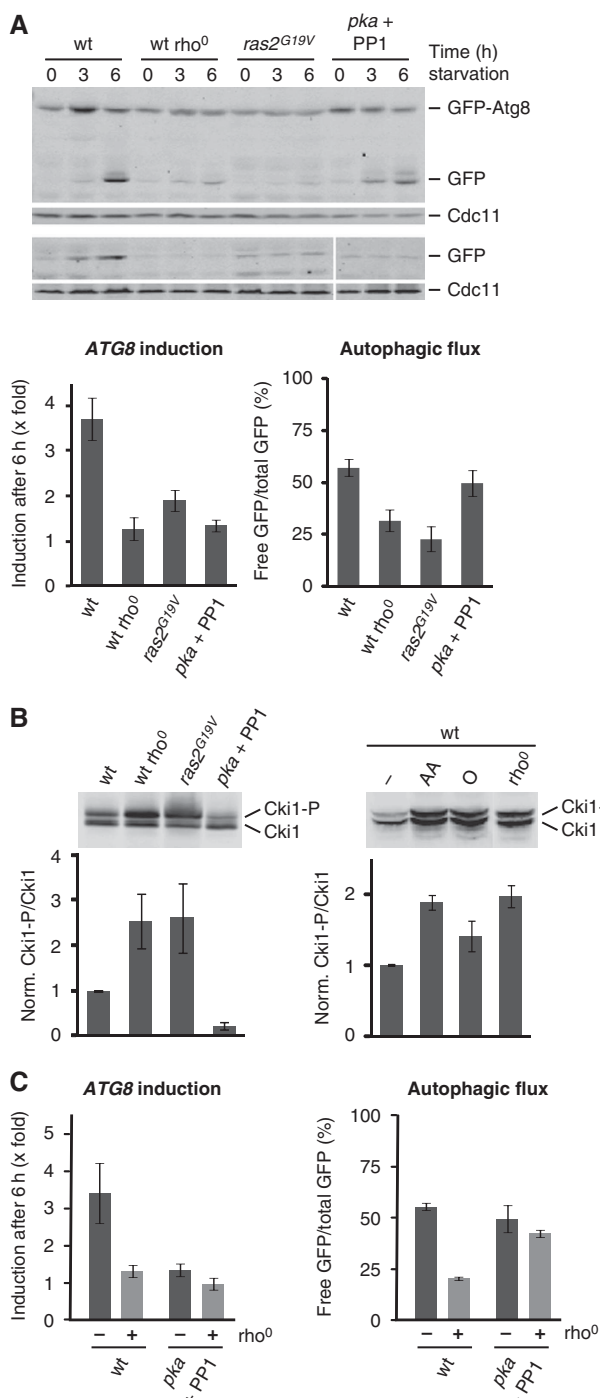
response. Specifically, we engineered cells that express a constitutively active variant of *RAS2* (*ras2<sup>G19V</sup>*), which results in hyperactivation of PKA (Toda *et al.*, 1985; Budovskaya *et al.*, 2004). Additionally, we used cells that express variants of the three catalytic subunits of PKA (*pka: tpk1<sup>M164G</sup>, tpk2<sup>M147G</sup>, tpk3<sup>M165G</sup>*) instead of the wild-type alleles, which are sensitive to conditional inactivation by the inhibitor 1NM-PP1 (PP1) (Yorimitsu *et al.*, 2007). We compared the autophagic response in these strains to wild-type and  $\rho^0$  cells under amino-acid starvation. Consistent with previous reports, expression of the constitutively active *ras2<sup>G19V</sup>* mutant inhibited the autophagic response (Figure 5A) (Budovskaya *et al.*, 2004). Remarkably, autophagic flux and *ATG8* induction were impaired to a similar extent as observed for  $\rho^0$  cells (Figure 5A), indicating that hyperactivation of PKA and mitochondrial respiratory deficiency lead to indistinguishable inhibition of the autophagy flux and *ATG8* induction component of the autophagic response. Inhibition of PKA activity (*pka* + PP1) did not significantly influence autophagic flux, but, surprisingly, impaired *ATG8* induction as observed in  $\rho^0$  or *ras2<sup>G19V</sup>*-expressing cells (Figure 5A). Thus, some level of PKA activity is required for full *ATG8* induction in wild-type cells under amino-acid starvation.

These data raise the possibility that mitochondria regulate the autophagic response in a manner dependent on PKA activity. To test this, we measured PKA activity *in vivo* in wild-type, wild-type  $\rho^0$ , *ras2<sup>G19V</sup>*-expressing, and *pka* (+ PP1) cells, or in wild-type cells in the presence of antimycin A or oligomycin using a PKA substrate reporter, which was created from a native substrate protein, Cki1 (Deminoff *et al.*, 2006). This PKA substrate reporter contains the first 200 amino acids of Cki1 and possesses mutations at two known protein kinase C sites (S125A, S130A) making its phosphorylation exclusively PKA dependent (S185). We detected PKA-dependent phosphorylation of the Cki1 reporter by a mobility shift in SDS-PAGE analysis and quantified the ratio of phosphorylated and unphosphorylated forms as a measure for the *in vivo* activity of PKA in cells during log-phase in synthetic galactose medium. As expected, we observed a decrease in the phosphorylated Cki1-P form upon inactivation of PKA (*pka* + PP1) compared with wild-type cells (Figure 5B). Remarkably, in  $\rho^0$  cells and wild-type cells treated with antimycin A, we observed a two-fold increase in the Cki1-P/Cki1 ratio relative to wild-type cells, similar to what we detected in cells with hyperactive PKA (*ras2<sup>G19V</sup>*) (Figure 5B). Interestingly, PKA activity was only mildly increased in wild-type cells in the presence of oligomycin, consistent with its relatively small inhibitory effects on the autophagic response (Figures 2B and 5B). These data demonstrate that the *in vivo* activity of PKA is modulated by mitochondrial function and that mitochondrial respiratory deficiency acts as a positive regulator of PKA. In this context, it is interesting to note that the PKA pathway has been previously shown to regulate mitochondrial function (Chevtzoff *et al.*, 2005; Chen and Powers, 2006). Thus, our findings suggest that mitochondria and PKA affect each other reciprocally, possibly to allow for adaptation of cell metabolism. Moreover, our data suggest that inhibition of *ATG8* induction and autophagic flux in wild-type cells in the presence of antimycin A or  $\rho^0$  cells is caused by an increase in PKA activity triggered by mitochondrial respiratory deficiency.



We tested whether inhibition of PKA activity reversed the defects in the autophagic response in cells with mitochondrial dysfunction by analysing  $\rho^0$  cells harbouring analogue-sensitive *pka* alleles under amino-acid starvation in the presence of 1NM-PP1. As we previously observed, both components of the autophagic response were stimulated in wild-type cells (Figure 5C). The addition of 1NM-PP1 to analogue-sensitive wild-type cells (*pka*) inhibited *ATG8* induction, but autophagic flux was stimulated in a manner similar to wild-type cells (Figure 5C). Importantly, in contrast to  $\rho^0$  cells, a strong stimulation of autophagic flux was observed in the presence of 1NM-PP1 in analogue-sensitive *pka*  $\rho^0$  cells (Figure 5C). These observations are consistent

with our hypothesis that mitochondrial respiratory deficiency stimulates PKA, which in turn suppresses autophagic flux in  $\rho^0$  cells. In contrast to autophagic flux, however, we did not observe stimulation in *ATG8* induction upon addition of 1NM-PP1 to analogue-sensitive *pka*  $\rho^0$  cells (Figure 5C). This observation is consistent with our previous finding that *ATG8* induction requires some baseline level of PKA activity in wild-type cells (Figure 5A) and suggests that a similar PKA requirement exists in cells with mitochondrial dysfunction. Our data suggest that mitochondrial function controls the autophagic response by modulating PKA activity, which in turn regulates both arms of the autophagic response—autophagic flux and *ATG8* induction—under amino-acid starvation.



### In the autophagic flux response, mitochondrial respiratory deficiency impairs Atg1–Atg13 complex recruitment to the PAS

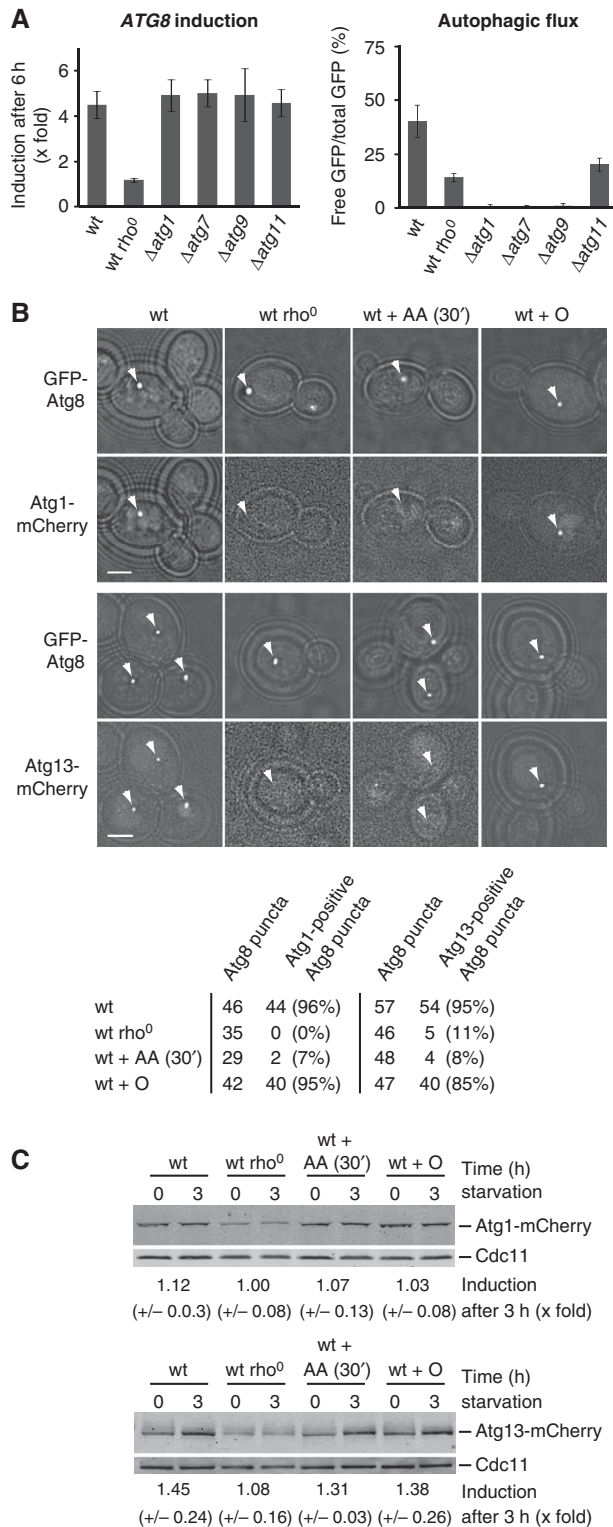
TORC1 and PKA regulate the Atg1–Atg13 complex, which in turn is a key regulator of the initial steps in autophagosome formation (Kamada *et al*, 2000; Cheong *et al*, 2008). First, we addressed whether *ATG8* induction and autophagic flux depend on the Atg1–Atg13 complex and whether *ATG8* induction and autophagic flux are interdependent events. Towards this goal, we analysed the autophagic response in  $\Delta atg1$ ,  $\Delta atg7$ , and  $\Delta atg9$  cells and  $\Delta atg11$  cells, which lack essential factors for general and selective autophagy, respectively (Lang *et al*, 2000; Kim *et al*, 2001). Significantly, autophagic flux was completely blocked in  $\Delta atg1$ ,  $\Delta atg7$ , or  $\Delta atg9$  cells (Figure 6A). We also observed a partial inhibition in autophagic flux in  $\Delta atg11$  cells during amino-acid starvation, indicating that Atg11 has a more general role during amino-acid starvation. However, *ATG8* induction was unaffected in all tested *ATG* mutants (Figure 6A). Thus, during amino-acid starvation, the Atg1–Atg13 complex is required for autophagic flux regulation, but dispensable for *ATG8* induction. In addition, *ATG8* induction is not dependent on the autophagy machinery required for autophagic flux. These findings are consistent with the existence of two independent regulatory arms of the autophagic response pathway.

To determine the basis for mitochondrial regulation of autophagic flux, we exploited the observation that PKA-dependent phosphorylation of Atg1 and Atg13 regulates

**Figure 5** Mitochondrial function controls autophagy by modulating PKA activity. (A) PKA-dependent regulation of the autophagic response under amino-acid starvation. Wild-type,  $\rho^0$ , *pka*, and *ras2<sup>G19V</sup>*-expressing cells harbouring pr<sup>ATG8</sup>-GFP-ATG8 (upper panels) or pr<sup>ATG8</sup>-GFP (lower panels) were exposed to amino-acid starvation medium supplemented with galactose. PKA activity in *pka* was inhibited by addition of 1NM-PP1 (PP1; 1  $\mu$ g/ml). Samples were analysed as described in Figure 1A; autophagic flux was determined after 3 and 6 h. (B) *In vivo* activity of PKA. Wild-type,  $\rho^0$ , *pka*, and *ras2<sup>G19V</sup>*-expressing cells harbouring 6xMYC-cki1<sup>2–200(S125/130A)</sup> (Cki1) were grown in galactose medium. When indicated, wild-type cells were grown in galactose medium in the presence of antimycin A (AA) or oligomycin (O) for 6 h. PKA-dependent phosphorylation of Cki1 was analysed by whole cell extraction and western blot analysis using a  $\alpha$ -Myc antibody (upper panels). Ratio of phosphorylated (Cki1-P) and non-phosphorylated (Cki1) forms of Cki1 relative to wild-type cells (wt = 1) (lower panels). (C) PKA inhibition restores autophagic flux, but not *ATG8* induction in the presence of mitochondrial dysfunction. Wild-type,  $\rho^0$ , *pka*, and *pka*  $\rho^0$  cells expressing pr<sup>ATG8</sup>-GFP-ATG8 were treated as described in (A). Samples were analysed as described in Figure 1A. The means and s.d. of four ( $n=4$ ) independent experiments are indicated in (A–C).

their localization to the PAS (Budovskaya *et al*, 2005; Stephan *et al*, 2009). Specifically, Atg1 and Atg13 are not recruited to the PAS in the presence of hyperactive PKA. Given that cells with mitochondrial respiratory deficiency display a strong increase in PKA *in vivo* activity (Figure 5B), we determined whether Atg1 and Atg13 localized to punctate structures labelled by GFP-Atg8, which are likely the PAS during amino-acid starvation under conditions of mitochondrial

dysfunction. In wild-type cells, GFP-Atg8 and Atg1-mCherry or GFP-Atg8 and Atg13-mCherry co-localized in the majority of puncta under amino-acid starvation conditions, consistent with a stimulation of the autophagic response (Figure 6B). Although GFP-Atg8 puncta were present at similar frequency (50–75% of the cells;  $n \geq 150$ ) in  $\rho^0$  or antimycin A-treated wild-type cells as compared with wild-type cells, there was a significant decrease in Atg1- or Atg13-mCherry-positive Atg8 puncta at these structures (Figure 6B). In contrast, Atg1- or Atg13-mCherry co-localized with GFP-Atg8 in the presence of oligomycin during amino-acid starvation to an extent similar to that observed in wild-type cells consistent with the smaller increase in PKA activity observed as compared with  $\rho^0$  or antimycin A-treated wild-type cells (Figures 5B and 6B). Under all conditions, Atg1-mCherry was present at comparable steady-state levels in cells as monitored by western analysis (Figure 6C). The expression of Atg13-mCherry was induced  $\approx 1.5$ -fold in wild-type cells (Figure 6C). This induction was inhibited in  $\rho^0$  cells, but it was comparable with wild-type cells in antimycin A-treated or oligomycin-treated cells (Figure 6C). These findings suggest that mislocalization of Atg13 observed in response to mitochondrial dysfunction is a consequence of PKA regulation rather than protein levels. Thus, during amino-acid starvation, our data suggest that even short-term mitochondrial respiratory deficiency strongly impairs the recruitment of Atg1 or Atg13 to the PAS, consistent with our observations that mitochondrial respiratory deficiency increases PKA activity and impairs autophagic flux under these conditions. Taken together, these data are consistent with a model in which mitochondrial respiratory deficiency induces PKA activity and, thereby, suppresses the two arms of autophagy regulation: induction of critical ATG components like Atg8 and Atg14 and organization of the PAS required for autophagic flux.



## Discussion

Our data demonstrate that mitochondrial function is a critical regulator of autophagy in *S. cerevisiae* and support the model summarized in Figure 7. Our data indicate that the autophagy response to amino-acid starvation is controlled by at least two components, autophagic flux and ATG gene induction,

**Figure 6** Mitochondrial respiratory deficiency impairs PAS recruitment of the Atg1-Atg13 complex under amino-acid starvation. **(A)** ATG8 induction is independent of the Atg1-Atg13 complex and autophagic flux. Wild-type,  $\rho^0$ ,  $\Delta atg1$ ,  $\Delta atg7$ ,  $\Delta atg9$ , and  $\Delta atg11$  cells harbouring  $pr^{ATG8}$ -GFP-ATG8 were analysed as described in Figure 1A. The means and s.d. of four ( $n = 4$ ) independent experiments are indicated. **(B)** Atg1 and Atg13 recruitment to the PAS depends on mitochondrial function. Wild-type and  $\rho^0$  cells harbouring  $pr^{ATG8}$ -GFP-ATG8 and  $pr^{ATG1}$ -ATG1-mCherry (upper panels) or  $pr^{ATG13}$ -ATG13-mCherry (lower panels) were exposed to amino-acid starvation medium supplemented with galactose for 3 h. Wild-type cells were treated with antimycin A (AA 30') after 2.5 h of starvation for 30 min or with oligomycin (O) for 3 h of starvation. Arrowheads indicate the position of GFP-Atg8 puncta. Transmission and fluorescence light microscopy images were superimposed to visualize cellular boundaries. Scale bar represents 1.5  $\mu$ m. **(C)** Steady-state levels of Atg1- and Atg13-mCherry during amino-acid starvation. Wild-type,  $\rho^0$ , and  $\Delta atg7$  cells expressing  $pr^{ATG1}$ -ATG1-mCherry (upper panels) or  $pr^{ATG13}$ -ATG13-mCherry (lower panels) were exposed and treated as described in **(B)** and analysed by whole cell extraction and western blot analysis using  $\alpha$ -dsRed and  $\alpha$ -Cdc11 antibodies.

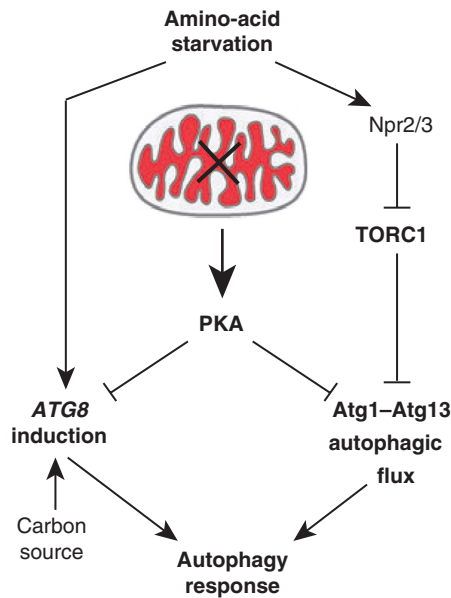


**Figure 7** Model for the role of mitochondrial function in autophagy regulation under amino-acid starvation. Amino-acid starvation induces the two regulatory arms of the autophagic response, *ATG8* induction and autophagic flux. Autophagic flux is regulated in an Atg1, PKA, and TORC1-dependent manner, while *ATG8* induction is regulated by PKA. Mitochondrial respiratory deficiency induces PKA activity and, thereby, suppresses both arms of the autophagic response.

and are consistent with previously published data (Abeliovich *et al*, 2000). Interestingly, these two components are differentially regulated. Our data together with published work indicate that the autophagic flux component is controlled by the Atg1-Atg13 complex and is negatively regulated by independent phosphorylation by both TORC1 and PKA (Funakoshi *et al*, 1997; Matsuura *et al*, 1997; Kamada *et al*, 2000, 2010; Budovskaya *et al*, 2005; Stephan *et al*, 2009). The *ATG* gene induction component, specifically *ATG8*, modulates the magnitude of the autophagic response by controlling the size of the autophagic compartment (Abeliovich *et al*, 2000; Xie *et al*, 2008). In contrast to autophagic flux, our data indicate that *ATG8* induction is negatively controlled by PKA in an Atg1- and TORC1-independent manner. Importantly, within this autophagy regulatory network, mitochondrial respiratory function is a critical modulator of PKA activity and regulates both the autophagic flux and *ATG8* induction components of the autophagy pathway.

TOR and PKA function together to coordinate nutrient availability with cell proliferation and growth in eukaryotic cells (Dechant and Peter, 2008; Zaman *et al*, 2008). PKA transitions cells from aerobic respiration to fermentative growth via the suppression of genes associated with mitochondrial activity (Chen and Powers, 2006; Dechant and Peter, 2008; Zaman *et al*, 2008). Our observation that mitochondrial dysfunction activates PKA in cells suggests that a reciprocal relationship exists between PKA activity and mitochondrial function. The physiological role of this regulatory circuit likely insures that cellular metabolism adapts to fermentation in response to respiratory deficiency. The circuit may also function to lower mitochondrial stress by suppressing the synthesis and import of new mitochondrial proteins so that the mitochondrial protein quality control systems can

be devoted to the maintenance of existing proteins. Lowering stress would provide a window of time for recovery, similar to other stress responses, such as the unfolded protein response in the endoplasmic reticulum (Ron and Walter, 2007). In this context, the suppression of autophagy by mitochondrial dysfunction would be another facet in this putative stress pathway. Alternatively, the degradation of cellular components might be disadvantageous under conditions where ATP can be solely generated by glycolysis and PKA activation in response to mitochondrial dysfunction might insure adaptation of the autophagic response to the metabolic capacity of the cell.

One key question is how mitochondrial respiratory deficiency signals to PKA. Our data indicate that the generation of mitochondrial membrane potential by respiration is a critical factor for autophagy induction and might signal the functional state of mitochondria. Consistently, under these conditions, we find the strongest increase in cellular PKA activity. It is interesting that in both mammalian and yeast cells depolarized mitochondria can induce selective autophagic turnover (mitophagy), consistent with a quality control mechanism (Priault *et al*, 2005; Nowikovsky *et al*, 2007; Narendra *et al*, 2008; Twig *et al*, 2008). However, our data indicate that mitochondrial respiratory deficiency inhibits general and selective autophagy, including mitophagy under amino-acid starvation (Supplementary Figure S7). Hence, the consequences of mitochondrial dysfunction on autophagy and mitophagy regulation can substantially vary depending on the nature and severity of the defects, for example collapse of mitochondrial membrane potential versus respiratory deficiency, as well as growth conditions in eukaryotic cells. Furthermore, our findings suggest that the accumulation of respiratory-deficient mitochondria beyond a certain threshold decreases the autophagic and mitophagic capacity of the cell and initiates a negative feedback loop that ultimately results in cellular ageing or cell death and might contribute to or initiate age-related diseases. A similar principle has been proposed for the collapse of the proteostasis capacity during ageing in *Caenorhabditis elegans* (Ben-Zvi *et al*, 2009), suggesting a common interdependence of cell metabolism, stress responses, and quality control mechanisms. While this model remains speculative at this point, it is interesting to note that TORC1 inhibition can alleviate effects on autophagic flux in the presence of respiratory-deficient mitochondria in our system. This is consistent with numerous reports on beneficial effects of modulated TOR activity for life span and age-related diseases across species (Kapahi *et al*, 2010). It is interesting to note that in fly neurons during ageing, the expression of several essential autophagy genes including Atg8a declines (Simonsen *et al*, 2008). This raises the possibility that in neurons mitochondrial dysfunction might compromise *ATG8* expression in ageing animal models in a similar manner to what we observe in yeast. Indeed, increased Atg8a expression can reverse neuronal damage and shortened life span, suggesting that Atg8a levels are rate limiting under these conditions (Simonsen *et al*, 2008). In this context, our findings, which indicate an interrelation of two common risk factors, mitochondrial dysfunction and impaired autophagy, may transform our understanding of the mechanism underlying ageing, cancerogenesis, and neurodegenerative diseases by raising the possibility of a common pathogenic mechanism.

## Materials and methods

### Cloning and plasmids

pRS416-pr<sup>ATG8</sup>-GFP-ATG8 has been described previously (Abeliovich *et al*, 2003). pRS426-pr<sup>ATG8</sup>-GFP was generated by cloning an *EcoRI* and *HindIII* flanked pr<sup>ATG8</sup>-GFP fragment from pRS416-pr<sup>ATG8</sup>-GFP-ATG8 into pRS426. pRS426-pr<sup>ATG14</sup>-GFP was generated by cloning pr<sup>ATG14</sup> (–1000 to –1 bp 5'-region) flanked by *EcoRI* and *PstI* into pRS426 with *PstI* and *XmaI* flanked GFP. pRS314-pr<sup>ATG1</sup>-ATG1-mCherry and pRS314-pr<sup>ATG13</sup>-ATG13-mCherry were generated by cloning pr<sup>ATG1</sup>-ATG1 (–800 to –1 bp 5'-region plus ORF without stop codon) flanked by *NotI* and *BamHI* or pr<sup>ATG13</sup>-ATG13 (–1000 to –1 bp 5'-region plus ORF without stop codon) flanked by *NotI* and *XmaI* into pRS314 containing mCherry (Shaner *et al*, 2004), respectively. pRS314-pr<sup>NPR1</sup>-NPR1-HA was generated by cloning pr<sup>NPR1</sup>-NPR1 (–763 to –1 bp 5'-region plus ORF without stop codon) containing a single HA tag flanked by *SacI* and *XmaI* into pRS314. pCM184-ras2<sup>G19V</sup> was generated by cloning RAS2 flanked by *BamHI* and *NotI* into pCM184 (Gari *et al*, 1997), and mutation G19V was introduced by site-directed mutagenesis. pRS416-pr<sup>OM45</sup>-OM45-GFP was generated by cloning pr<sup>OM45</sup>-OM45 (–878 to –1 bp 5'-region plus ORF without stop codon) flanked by *NotI* and *BamHI* into pRS416 with *BamHI* and *EcoRI* flanked GFP. pRS423-pr<sup>CUP</sup>-6xMYC-ckl1<sup>2–200(S125/130A)</sup> was generated as described in Deminoff *et al* (2006) and mutations S125/130A were introduced by mutagenesis PCR (kind gift from Dr Paul Herman).

### Yeast strains and media

All strains used in this study are derivatives of W303 (*leu2-3,112*; *ura3-1*; *his3-11,15*; *trp1-1*; *ade2-1*; *can1-100*). Gene deletions were generated by PCR-based targeted homologous recombination replacing complete ORFs by *kanMX6* (*Δatg1*, *Δatg7*, *Δatg9*), *natMX* (*Δchs1*, *Δmss51*, *Δpet111*, *Δpet122*, or *Δatp10*), or *HIS3MX6* (*Δatg11*, *Δatg32*, *Δnpr2*, *Δvma2*) cassettes (Longtine *et al*, 1998). The rho<sup>0</sup> strains were generated by growth in YPD medium supplemented with ethidium bromide (25 μg/ml). Strains were grown to log-phase in synthetic galactose medium (0.7% yeast nitrogen base, 2% galactose, and 0.05% glucose) or Ylactate medium (1% yeast extract, 2% peptone, and 2% lactate) and exposed to amino-acid (0.1% yeast extract) or nitrogen (-N; 0.17% yeast nitrogen base without (NH<sub>4</sub>)<sub>2</sub>SO<sub>4</sub> and amino acids) starvation medium supplemented with acetate (1%), galactose (2%), or glucose (2%) as indicated. Antimycin A (1 μg/ml), oligomycin (7.5 μg/ml), or rapamycin (400 ng/ml) was added when indicated. To suppress or allow expression, strains harbouring pCM184-ras2<sup>G19V</sup> were grown in the presence or absence (12 h) of doxycyclin (20 μg/ml), respectively. The 1NM-PP1-sensitive *pka* (*tpk1*<sup>M164G</sup>, *tpk2*<sup>M147G</sup>, and *tpk3*<sup>M165G</sup>) strain has been described in Yorimitsu *et al* (2007). To block PKA activity, *pka* strains were pre-incubated (60 min) and starved in the presence of 1NM-PP1 (1 μg/ml) in indicated media. Strains harbouring pRS423-pr<sup>CUP</sup>-6xMYC-ckl1<sup>2–200(S125/130A)</sup> were grown in synthetic galactose medium as described in Deminoff *et al* (2006).

### Whole cell extraction, western blot analysis, and quantification

At indicated time points, cells corresponding to 0.25 OD<sub>600</sub> units were collected and lysed by alkaline whole cell extraction (0.255 M NaOH, 1% β-mercaptoethanol). Protein extracts were analysed by SDS-PAGE and immunoblotting (α-Atg13, polyclonal, Dr Klionsky; α-Cdc11, polyclonal, Novus Biologicals; α-dsRed, polyclonal, Clontech; α-GFP and α-HA, monoclonal, Covance; α-Myc, monoclonal, Sigma; α-Pgk1, monoclonal, Molecular Probes) and visualized with

the appropriate secondary antibodies conjugated to IRDye (800CW; LI-COR Biosciences). Quantification was performed using the Odyssey Infrared Imaging System (LI-COR Biosciences).

### Fluorescence microscopy

Cells were mounted in 0.5% low melt agarose in indicated starvation medium and viewed with a microscope (IX70 Delta-vision; Olympus) using a ×60 1.4 NA objective (Olympus) and a 100-W mercury lamp (Applied Precision, LLC). Two- and three-dimensional light microscopy data were collected using an integrated, cooled charge-coupled device-based camera (MicroMax; Princeton) equipped with an interline chip (Sony). Three-dimensional data sets were processed using DeltaVision's iterative, constrained three-dimensional deconvolution method to remove out of focus light. Representative sections of deconvolved images were processed in SoftWorx (Applied Precision, LLC) and PHOTOSHOP (Adobe Systems, San Jose, CA) software unless otherwise indicated.

### Measurement of cellular and mitochondrial ATP

At indicated time points, cells corresponding to 50 OD<sub>600</sub> units were collected, washed, and resuspended in 1 ml NMIB buffer (0.6 M sorbitol; 5 mM MgCl<sub>2</sub>; 50 mM KCl; 100 mM KOAc; 20 mM HEPES pH 7.4), and frozen in liquid nitrogen as droplets. Cell breakage was performed using the SPEX freezer mill 6750 (3 cycles; rate 7 for 2 min). After cell debris was removed from thawed cell powder by centrifugation, the protein concentration of the supernatant (total cell) was determined by a standard Bradford assay and 10 μl were mixed with 90 μl TCA (5%) for ATP determination using the promega ENLITEN® ATP assay, according to the instructions of the manufacturer. Mitochondria were isolated from total cell supernatant by differential centrifugation and resuspended in 25 μl NMIB buffer. The protein concentration was determined by a standard Bradford assay and 10 μl were mixed with 90 μl TCA (5%) for ATP determination.

### Measurement of mitochondrial membrane potential

After 3 h of amino-acid starvation, cells were exposed to 3,3'-dihexyloxycarbocyanine iodide (DiOC<sub>3</sub>(6)) (10 ng/ml final concentration) for 5 min at 23°C. Three-dimensional data sets of cells with identical exposure times (1 s) and intensity scales were collected. For analysis, pixel intensities for cross-sections of at least 10 mitochondrial tubules in 5 representative cells were determined using ImageJ software (NIH) for each condition.

### Supplementary data

Supplementary data are available at *The EMBO Journal* Online (<http://www.embojournal.org>).

## Acknowledgements

We thank Dr Paul Herman and Dr Dan Klionsky for providing constructs, antibodies, and yeast strains and Dr Ted Powers as well as members of the Nunnari laboratory for critical discussion and comments. JN is supported by NIH Grant R01GM062942.

*Author contributions:* MG and JN designed the study and wrote the manuscript. MG performed all experiments and analysed the data.

## Conflict of interest

The authors declare that they have no conflict of interest.

## References

- Abeliovich H, Dunn Jr WA, Kim J, Klionsky DJ (2000) Dissection of autophagosome biogenesis into distinct nucleation and expansion steps. *J Cell Biol* **151**: 1025–1034
- Abeliovich H, Zhang C, Dunn Jr WA, Shokat KM, Klionsky DJ (2003) Chemical genetic analysis of Apg1 reveals a non-kinase role in the induction of autophagy. *Mol Biol Cell* **14**: 477–490
- Ackerman SH, Tzagoloff A (1990) ATP10, a yeast nuclear gene required for the assembly of the mitochondrial F1-F0 complex. *J Biol Chem* **265**: 9952–9959
- Banerjee R, Starkov AA, Beal MF, Thomas B (2009) Mitochondrial dysfunction in the limelight of Parkinson's disease pathogenesis. *Biochim Biophys Acta* **1792**: 651–663
- Ben-Zvi A, Miller EA, Morimoto RI (2009) Collapse of proteostasis represents an early molecular event in *Caenorhabditis elegans* aging. *Proc Natl Acad Sci USA* **106**: 14914–14919
- Budovskaya YV, Stephan JS, Deminoff SJ, Herman PK (2005) An evolutionary proteomics approach identifies substrates of the cAMP-dependent protein kinase. *Proc Natl Acad Sci USA* **102**: 13933–13938



- Budovskaya YV, Stephan JS, Reggiori F, Klionsky DJ, Herman PK (2004) The Ras/cAMP-dependent protein kinase signaling pathway regulates an early step of the autophagy process in *Saccharomyces cerevisiae*. *J Biol Chem* **279**: 20663–20671
- Cardoso SM, Pereira CF, Moreira PI, Arduino DM, Esteves AR, Oliveira CR (2010) Mitochondrial control of autophagic lysosomal pathway in Alzheimer's disease. *Exp Neurol* **223**: 294–298
- Cebollero E, Reggiori F (2009) Regulation of autophagy in yeast *Saccharomyces cerevisiae*. *Biochim Biophys Acta* **1793**: 1413–1421
- Chan EY, Kir S, Tooze SA (2007) siRNA screening of the kinome identifies ULK1 as a multidomain modulator of autophagy. *J Biol Chem* **282**: 25464–25474
- Chan TF, Bertram PG, Ai W, Zheng XF (2001) Regulation of APG14 expression by the GATA-type transcription factor Gln3p. *J Biol Chem* **276**: 6463–6467
- Chen JC, Powers T (2006) Coordinate regulation of multiple and distinct biosynthetic pathways by TOR and PKA kinases in *S cerevisiae*. *Curr Genet* **49**: 281–293
- Chen LB (1988) Mitochondrial membrane potential in living cells. *Annu Rev Cell Biol* **4**: 155–181
- Chen S, Tarsio M, Kane PM, Greenberg ML (2008) Cardiolipin mediates cross-talk between mitochondria and the vacuole. *Mol Biol Cell* **19**: 5047–5058
- Cheong H, Nair U, Geng J, Klionsky DJ (2008) The Atg1 kinase complex is involved in the regulation of protein recruitment to initiate sequestering vesicle formation for nonspecific autophagy in *Saccharomyces cerevisiae*. *Mol Biol Cell* **19**: 668–681
- Chevtzoff C, Vallortigara J, Averet N, Rigoulet M, Devin A (2005) The yeast cAMP protein kinase Tpk3p is involved in the regulation of mitochondrial enzymatic content during growth. *Biochim Biophys Acta* **1706**: 117–125
- Costanzo MC, Fox TD (1988) Specific translational activation by nuclear gene products occurs in the 5' untranslated leader of a yeast mitochondrial mRNA. *Proc Natl Acad Sci USA* **85**: 2677–2681
- Dechant R, Peter M (2008) Nutrient signals driving cell growth. *Curr Opin Cell Biol* **20**: 678–687
- Decoster E, Simon M, Hatat D, Faye G (1990) The MSS51 gene product is required for the translation of the COX1 mRNA in yeast mitochondria. *Mol Gen Genet* **224**: 111–118
- Deminoff SJ, Howard SC, Hester A, Warner S, Herman PK (2006) Using substrate-binding variants of the cAMP-dependent protein kinase to identify novel targets and a kinase domain important for substrate interactions in *Saccharomyces cerevisiae*. *Genetics* **173**: 1909–1917
- Ecker N, Mor A, Journo D, Abeliovich H (2010) Induction of autophagic flux by amino acid deprivation is distinct from nitrogen starvation-induced macroautophagy. *Autophagy* **6**: 879–890
- Funakoshi T, Matsuura A, Noda T, Ohsumi Y (1997) Analyses of APG13 gene involved in autophagy in yeast, *Saccharomyces cerevisiae*. *Gene* **192**: 207–213
- Galluzzi L, Morselli E, Kepp O, Vitale I, Rigoni A, Vacchelli E, Michaud M, Zischka H, Castedo M, Kroemer G (2010) Mitochondrial gateways to cancer. *Mol Aspects Med* **31**: 1–20
- Gander S, Bonenfant D, Altermatt P, Martin DE, Hauri S, Moes S, Hall MN, Jenoe P (2008) Identification of the rapamycin-sensitive phosphorylation sites within the Ser/Thr-rich domain of the yeast Npr1 protein kinase. *Rapid Commun Mass Spectrom* **22**: 3743–3753
- Gari E, Piedrafita L, Aldea M, Herrero E (1997) A set of vectors with a tetracycline-regulatable promoter system for modulated gene expression in *Saccharomyces cerevisiae*. *Yeast* **13**: 837–848
- Geisler S, Holmstrom KM, Skujat D, Fiesel FC, Rothfuss OC, Kahle PJ, Springer W (2010) PINK1/Parkin-mediated mitophagy is dependent on VDAC1 and p62/SQSTM1. *Nat Cell Biol* **12**: 119–131
- Graham LA, Powell B, Stevens TH (2000) Composition and assembly of the yeast vacuolar H(+)-ATPase complex. *J Exp Biol* **203**: 61–70
- Hara T, Nakamura K, Matsui M, Yamamoto A, Nakahara Y, Suzuki-Migishima R, Yokoyama M, Mishima K, Saito I, Okano H, Mizushima N (2006) Suppression of basal autophagy in neural cells causes neurodegenerative disease in mice. *Nature* **441**: 885–889
- Hara T, Takamura A, Kishi C, Iemura S, Natsume T, Guan JL, Mizushima N (2008) FIP200, a ULK-interacting protein, is required for autophagosome formation in mammalian cells. *J Cell Biol* **181**: 497–510
- Hardwick JS, Kuruvilla FG, Tong JK, Shamji AF, Schreiber SL (1999) Rapamycin-modulated transcription defines the subset of nutrient-sensitive signaling pathways directly controlled by the Tor proteins. *Proc Natl Acad Sci USA* **96**: 14866–14870
- He C, Klionsky DJ (2009) Regulation mechanisms and signaling pathways of autophagy. *Annu Rev Genet* **43**: 67–93
- Herrmann JM, Funes S (2005) Biogenesis of cytochrome oxidase-sophisticated assembly lines in the mitochondrial inner membrane. *Gene* **354**: 43–52
- Huang J, Klionsky DJ (2007) Autophagy and human disease. *Cell Cycle* **6**: 1837–1849
- Huang WP, Scott SV, Kim J, Klionsky DJ (2000) The itinerary of a vesicle component, Aut7p/Cvt5p, terminates in the yeast vacuole via the autophagy/Cvt pathways. *J Biol Chem* **275**: 5845–5851
- Johnson LV, Walsh ML, Bockus BJ, Chen LB (1981) Monitoring of relative mitochondrial membrane potential in living cells by fluorescence microscopy. *J Cell Biol* **88**: 526–535
- Kabeya Y, Kamada Y, Baba M, Takikawa H, Sasaki M, Ohsumi Y (2005) Atg17 functions in cooperation with Atg1 and Atg13 in yeast autophagy. *Mol Biol Cell* **16**: 2544–2553
- Kamada Y, Funakoshi T, Shintani T, Nagano K, Ohsumi M, Ohsumi Y (2000) Tor-mediated induction of autophagy via an Apg1 protein kinase complex. *J Cell Biol* **150**: 1507–1513
- Kamada Y, Yoshino KI, Kondo C, Kawamata T, Oshiro N, Yonezawa K, Ohsumi Y (2010) Tor directly controls the Atg1 kinase complex to regulate autophagy. *Mol Cell Biol* **30**: 1049–1058
- Kanki T, Klionsky DJ (2008) Mitophagy in yeast occurs through a selective mechanism. *J Biol Chem* **283**: 32386–32393
- Kanki T, Wang K, Cao Y, Baba M, Klionsky DJ (2009) Atg32 is a mitochondrial protein that confers selectivity during mitophagy. *Dev Cell* **17**: 98–109
- Kapahi P, Chen D, Rogers AN, Katewa SD, Li PW, Thomas EL, Kockel L (2010) With TOR, less is more: a key role for the conserved nutrient-sensing TOR pathway in aging. *Cell Metab* **11**: 453–465
- Kawamata T, Kamada Y, Kabeya Y, Sekito T, Ohsumi Y (2008) Organization of the pre-autophagosomal structure responsible for autophagosome formation. *Mol Biol Cell* **19**: 2039–2050
- Kim J, Kamada Y, Stromhaug PE, Guan J, Hefner-Gravink A, Baba M, Scott SV, Ohsumi Y, Dunn Jr WA, Klionsky DJ (2001) Cvt9/Gsa9 functions in sequestering selective cytosolic cargo destined for the vacuole. *J Cell Biol* **153**: 381–396
- Kirisako T, Baba M, Ishihara N, Miyazawa K, Ohsumi M, Yoshimori T, Noda T, Ohsumi Y (1999) Formation process of autophagosome is traced with Apg8/Aut7p in yeast. *J Cell Biol* **147**: 435–446
- Kissova I, Deffieu M, Manon S, Camougrand N (2004) Uth1p is involved in the autophagic degradation of mitochondria. *J Biol Chem* **279**: 39068–39074
- Kissova I, Salin B, Schaeffer J, Bhatia S, Manon S, Camougrand N (2007) Selective and non-selective autophagic degradation of mitochondria in yeast. *Autophagy* **3**: 329–336
- Komatsu M, Waguri S, Chiba T, Murata S, Iwata J, Tanida I, Ueno T, Koike M, Uchiyama Y, Kominami E, Tanaka K (2006) Loss of autophagy in the central nervous system causes neurodegeneration in mice. *Nature* **441**: 880–884
- Komatsu M, Waguri S, Ueno T, Iwata J, Murata S, Tanida I, Ezaki J, Mizushima N, Ohsumi Y, Uchiyama Y, Kominami E, Tanaka K, Chiba T (2005) Impairment of starvation-induced and constitutive autophagy in Atg7-deficient mice. *J Cell Biol* **169**: 425–434
- Lambert AJ, Brand MD (2009) Reactive oxygen species production by mitochondria. *Methods Mol Biol* **554**: 165–181
- Lang T, Reiche S, Straub M, Bredschneider M, Thumm M (2000) Autophagy and the cvt pathway both depend on AUT9. *J Bacteriol* **182**: 2125–2133
- Lee JH, Yu WH, Kumar A, Lee S, Mohan PS, Peterhoff CM, Wolfe DM, Martinez-Vicente M, Massey AC, Sovak G, Uchiyama Y, Westaway D, Cuervo AM, Nixon RA (2010) Lysosomal proteolysis and autophagy require presenilin 1 and are disrupted by Alzheimer-related PS1 mutations. *Cell* **141**: 1146–1158
- Longtine MS, McKenzie III A, Demarini DJ, Shah NG, Wach A, Brachat A, Philippsen P, Pringle JR (1998) Additional modules for versatile and economical PCR-based gene deletion and modification in *Saccharomyces cerevisiae*. *Yeast* **14**: 953–961
- Ludovico P, Sansonetty F, Corte-Real M (2001) Assessment of mitochondrial membrane potential in yeast cell populations by flow cytometry. *Microbiology* **147**: 3335–3343
- Matsuura A, Tsukada M, Wada Y, Ohsumi Y (1997) Apg1p, a novel protein kinase required for the autophagic process in *Saccharomyces cerevisiae*. *Gene* **192**: 245–250
- Meijer AJ, Codogno P (2009) Autophagy: regulation and role in disease. *Crit Rev Clin Lab Sci* **46**: 210–240

- Morselli E, Galluzzi L, Kepp O, Vicencio JM, Criollo A, Maiuri MC, Kroemer G (2009) Anti- and pro-tumor functions of autophagy. *Biochim Biophys Acta* **1793**: 1524–1532
- Nakamura N, Matsuura A, Wada Y, Ohsumi Y (1997) Acidification of vacuoles is required for autophagic degradation in the yeast, *Saccharomyces cerevisiae*. *J Biochem* **121**: 338–344
- Nakatogawa H, Suzuki K, Kamada Y, Ohsumi Y (2009) Dynamics and diversity in autophagy mechanisms: lessons from yeast. *Nat Rev Mol Cell Biol* **10**: 458–467
- Narendra D, Tanaka A, Suen DF, Youle RJ (2008) Parkin is recruited selectively to impaired mitochondria and promotes their autophagy. *J Cell Biol* **183**: 795–803
- Narendra DP, Jin SM, Tanaka A, Suen DF, Gautier CA, Shen J, Cookson MR, Youle RJ (2010) PINK1 is selectively stabilized on impaired mitochondria to activate parkin. *PLoS Biol* **8**: e1000298
- Neklesa TK, Davis RW (2009) A genome-wide screen for regulators of TORC1 in response to amino acid starvation reveals a conserved Npr2/3 complex. *PLoS Genet* **5**: e1000515
- Noda T, Ohsumi Y (1998) Tor, a phosphatidylinositol kinase homologue, controls autophagy in yeast. *J Biol Chem* **273**: 3963–3966
- Nowikovsky K, Reipert S, Devenish RJ, Schweyen RJ (2007) Mdm38 protein depletion causes loss of mitochondrial K<sup>+</sup>/H<sup>+</sup> exchange activity, osmotic swelling and mitophagy. *Cell Death Differ* **14**: 1647–1656
- Okamoto K, Kondo-Okamoto N, Ohsumi Y (2009) Mitochondria-anchored receptor Atg32 mediates degradation of mitochondria via selective autophagy. *Dev Cell* **17**: 87–97
- Petit P, Glab N, Marie D, Kieffer H, Metezeau P (1996) Discrimination of respiratory dysfunction in yeast mutants by confocal microscopy, image, and flow cytometry. *Cytometry* **23**: 28–38
- Poutre CG, Fox TD (1987) PET111, a *Saccharomyces cerevisiae* nuclear gene required for translation of the mitochondrial mRNA encoding cytochrome c oxidase subunit II. *Genetics* **115**: 637–647
- Priault M, Salin B, Schaeffer J, Vallette FM, di Rago JP, Martinou JC (2005) Impairing the bioenergetic status and the biogenesis of mitochondria triggers mitophagy in yeast. *Cell Death Differ* **12**: 1613–1621
- Rodel G (1997) Translational activator proteins required for cytochrome b synthesis in *Saccharomyces cerevisiae*. *Curr Genet* **31**: 375–379
- Ron D, Walter P (2007) Signal integration in the endoplasmic reticulum unfolded protein response. *Nat Rev Mol Cell Biol* **8**: 519–529
- Scherz-Shouval R, Shvets E, Fass E, Shorer H, Gil L, Elazar Z (2007) Reactive oxygen species are essential for autophagy and specifically regulate the activity of Atg4. *EMBO J* **26**: 1749–1760
- Schmidt A, Beck T, Koller A, Kunz J, Hall MN (1998) The TOR nutrient signalling pathway phosphorylates NPR1 and inhibits turnover of the tryptophan permease. *EMBO J* **17**: 6924–6931
- Shaner NC, Campbell RE, Steinbach PA, Giepmans BN, Palmer AE, Tsien RY (2004) Improved monomeric red, orange and yellow fluorescent proteins derived from *Discosoma* sp. red fluorescent protein. *Nat Biotechnol* **22**: 1567–1572
- Shintani T, Klionsky DJ (2004) Cargo proteins facilitate the formation of transport vesicles in the cytoplasm to vacuole targeting pathway. *J Biol Chem* **279**: 29889–29894
- Simonsen A, Cumming RC, Brech A, Isakson P, Schubert DR, Finley KD (2008) Promoting basal levels of autophagy in the nervous system enhances longevity and oxidant resistance in adult *Drosophila*. *Autophagy* **4**: 176–184
- Stephan JS, Yeh YY, Ramachandran V, Deminoff SJ, Herman PK (2009) The Tor and PKA signaling pathways independently target the Atg1/Atg13 protein kinase complex to control autophagy. *Proc Natl Acad Sci USA* **106**: 17049–17054
- Suen DF, Narendra DP, Tanaka A, Manfredi G, Youle RJ (2010) Parkin overexpression selects against a deleterious mtDNA mutation in heteroplasmic cybrid cells. *Proc Natl Acad Sci USA* **107**: 11835–11840
- Suzuki K, Kubota Y, Sekito T, Ohsumi Y (2007) Hierarchy of Atg proteins in pre-autophagosomal structure organization. *Genes Cells* **12**: 209–218
- Takeshige K, Baba M, Tsuboi S, Noda T, Ohsumi Y (1992) Autophagy in yeast demonstrated with proteinase-deficient mutants and conditions for its induction. *J Cell Biol* **119**: 301–311
- Tal R, Winter G, Ecker N, Klionsky DJ, Abeliovich H (2007) Aup1p, a yeast mitochondrial protein phosphatase homolog, is required for efficient stationary phase mitophagy and cell survival. *J Biol Chem* **282**: 5617–5624
- Tanida I, Mizushima N, Kiyooka M, Ohsumi M, Ueno T, Ohsumi Y, Kominami E (1999) Apg7p/Cvt2p: a novel protein-activating enzyme essential for autophagy. *Mol Biol Cell* **10**: 1367–1379
- Toda T, Uno I, Ishikawa T, Powers S, Kataoka T, Broek D, Cameron S, Broach J, Matsumoto K, Wigler M (1985) In yeast, RAS proteins are controlling elements of adenylate cyclase. *Cell* **40**: 27–36
- Tsukada M, Ohsumi Y (1993) Isolation and characterization of autophagy-defective mutants of *Saccharomyces cerevisiae*. *FEBS Lett* **333**: 169–174
- Twig G, Elorza A, Molina AJ, Mohamed H, Wikstrom JD, Walzer G, Stiles L, Haigh SE, Katz S, Las G, Alroy J, Wu M, Py BF, Yuan J, Deeney JT, Corkey BE, Shirihai OS (2008) Fission and selective fusion govern mitochondrial segregation and elimination by autophagy. *EMBO J* **27**: 433–446
- Tzagoloff A, Barrientos A, Neupert W, Herrmann JM (2004) Atp10p assists assembly of Atp6p into the F0 unit of the yeast mitochondrial ATPase. *J Biol Chem* **279**: 19775–19780
- Vives-Bauza C, Zhou C, Huang Y, Cui M, de Vries RL, Kim J, May J, Tocilescu MA, Liu W, Ko HS, Magrane J, Moore DJ, Dawson VL, Grailhe R, Dawson TM, Li C, Tieu K, Przedborski S (2010) PINK1-dependent recruitment of Parkin to mitochondria in mitophagy. *Proc Natl Acad Sci USA* **107**: 378–383
- Wong E, Cuervo AM (2010) Autophagy gone awry in neurodegenerative diseases. *Nat Neurosci* **13**: 805–811
- Xie Z, Klionsky DJ (2007) Autophagosome formation: core machinery and adaptations. *Nat Cell Biol* **9**: 1102–1109
- Xie Z, Nair U, Klionsky DJ (2008) Atg8 controls phagophore expansion during autophagosome formation. *Mol Biol Cell* **19**: 3290–3298
- Yang Z, Geng J, Yen WL, Wang K, Klionsky DJ (2010) Positive or negative roles of different cyclin-dependent kinase Pho85-cyclin complexes orchestrate induction of autophagy in *Saccharomyces cerevisiae*. *Mol Cell* **38**: 250–264
- Yorimitsu T, He C, Wang K, Klionsky DJ (2009) Tap42-associated protein phosphatase type 2A negatively regulates induction of autophagy. *Autophagy* **5**: 616–624
- Yorimitsu T, Zaman S, Broach JR, Klionsky DJ (2007) Protein kinase A and Sch9 cooperatively regulate induction of autophagy in *Saccharomyces cerevisiae*. *Mol Biol Cell* **18**: 4180–4189
- Zaman S, Lippman SI, Zhao X, Broach JR (2008) How *Saccharomyces* responds to nutrients. *Annu Rev Genet* **42**: 27–81